ARTICLE

Highly Selective Recognition of Al^{3+} and I[-] ions using a Bi-functional Fluorescent Probe †

Zhao Li,‡[a] Jiang-Lin Zhao,‡[b] Yu-Tian Wu,[a] Lan Mu,[a] Xi Zeng,*[a] Zongwen Jin,*[b] Gang Wei,*[c] Ning Xie[e] and Carl Redshaw[d]

A tripodal fluorescent probe **L1** armed with rhodamine B and 1-naphthaleneisothiocyanates was prepared in high yield. A study of the recognition properties revealed that probe **L1** exhibited high sensitivity and selectivity towards Al^{3+} through a "FRET" fluorescence response and colorimetric response with low detection limits of the order of 10^{-8} M. Meanwhile, probe **L1** also possessed high recognition capability for I[-] through fluorescent decay, which given there are comparatively few selective fluorescent probes for I[-], is significant. Furthermore, the complexation mechanisms were fully investigated by spectral titrations, ^{1}H NMR spectroscopic titrations and mass spectrometry. The utility of probe **L1** as a biosensor in living cells (PC3 cells) towards Al^{3+} ions has also been demonstrated.

Introduction

Aluminum, the third most abundant element in the lithosphere, is widely used in our daily life typically in aluminum-based pharmaceutical drugs, food additives and kitchen utensils[1] as well as in different industries including paper, textile, and water treatment.[2] However, Al^{3+} is not necessary for the human body, and was found to be neurotoxic to living organisms. According to the Food and Agriculture Organization and World Health Organization joint Expert Committee on Food Additives, the daily intake of Al^{3+} should not exceed 3–10 mg per day per kg body mass.[3] Indeed, an excessive intake of Al^{3+} into the human body may cause a variety of diseases such as myopathy, dementia, anemia, bone and joint diseases, as well as Alzheimer's and Parkinson's diseases.[4] Thus, the detection and quantification of Al^{3+} in environmental and living bio-systems is of great importance.

On the other hand, iodine is a critical micronutrient to produce indispensable thyroid hormones in human thyroid glands, which play fundamental physiological roles at all stages of human development from fetus to adulthood.[5] However, either iodide deficiency or excessive uptake can cause thyroid disorders. For example, a lack of sufficient iodine can typically lead to congenital anomalies, miscarriage and stillbirth.[6] In

contrast, an excessive uptake of iodine also results in negative effects, such as necrotic, degenerative, and neoplastic lesions in the thyroid gland, stomach and salivary glands.[7] Dasgupta has recently pointed out that nearly a third of the global population has suffered insufficient iodine intake and is at risk of developing iodine deficiency disorders.[8] Therefore, the robust detection of iodide is highly desirable. Unfortunately, comparatively few selective fluorescent probes for I[-] are currently available due to the iodide ion exhibiting the weakest binding capacity towards abiotic receptors owing to its large size *versus* other anions and poorest basicity amongst all the halide ions.[9] At the same time, the iodine ion is a fluorescence quenching heavy atom. Therefore, designing a satisfactory I[-] sensors still remains a big challenge.

Fluorescence probes are widely used as powerful tools for detecting ions owing to their high sensitivity, selectivity, rapid response rate, simplicity of manipulation and their capacity for real-time imaging and non-destructive nature.[10] In particular, bi-functional probes, which refer to those based on a single host that can independently recognize two guest species using distinct spectral responses[11], have already been reported and this is emerging as a promising research area. In view of the importance quantification of the Al^{3+} and I[-] ions, it is urgent to develop a bi-functional probe which has the capability to detect both Al^{3+} and I[-].

Herein, we introduce a tripodal bi-functional fluorescent probe (**L1**), which not only exhibits high selectivity for the Al^{3+} cation based on the FRET mechanism, but also high selectivity for I[-] anions based on fluorescent quenching accompanied by distinct colour changes. Moreover, fluorescent imaging experiments using live PC3 cells and the detection of intracellular Al^{3+} ions in living cells is also discussed herein.

[a.] Key Laboratory of Macrocyclic and Supramolecular Chemistry of Guizhou Province; School of Chemistry and Chemical engineering, Guizhou University, Guiyang 550025, China.

[b.] Shenzhen Institutes of Advanced Technology, Chinese Academy of Sciences, 1068 Xueyuan Avenue, Shenzhen 518055, China.

[c.] CSIRO Manufacturing Flagship, PO Box 218, NSW 2070, Australia.

[d.] Department of Chemistry, School of Mathematics and Physical Sciences, University of Hull, Hull HU6 7RX, U.K.

[e.] College of Life Science, Shenzhen Key Laboratory of Microbial Genetic Engineering, Shenzhen University, Shenzhen 518060, China
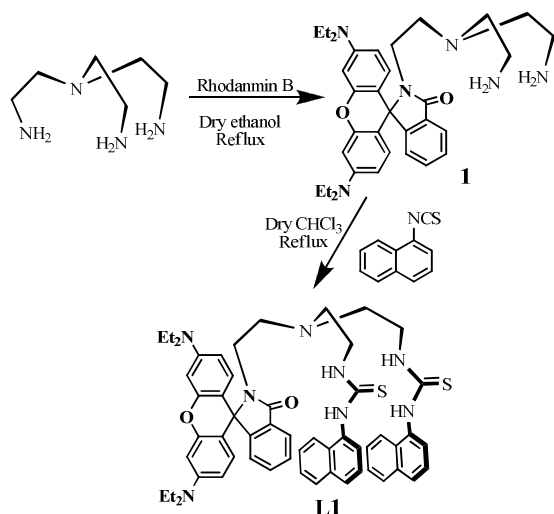
Scheme 1. The synthetic route to probe **L1**.

Results and discussion

Synthesis

The tripodal probe **L1** was prepared following the reported procedure with minor revisions in order to improve the yield (Scheme 1).[12] Rhodamine B was reacted with a large excess (8 equiv.) of tris(2-aminoethyl)amine to give the intermediate **1** in 87.3 % yield. Intermediate **1** was then coupled with two equiv. of 1-naphthaleneisothiocyanate in dry $CHCl_3$ at reflux overnight (24 h) to afford probe **L1** in 76.3 % yield (*cf* Ref. 12, 46 %). The structure of **L1** was fully elucidated by FT-IR, ^{1}H and ^{13}C NMR spectroscopy as well as mass spectrometry (Figs. S1-S6).

Recognition properties of probe L1 towards cations

Both fluorescence and UV-vis absorption spectroscopy were employed herein to investigate the recognition properties of probe **L1**. In H_2O/CH_3CN (10 μM, 2/98, v/v, pH = 7) solution, the fluorescence response of **L1** toward different metal ions was tested by exciting at 240 nm. Upon the addition of 20 equiv. of various ions (Li^+, Na^+, K^+, Ag^+, Mg^{2+}, Ca^{2+}, Ba^{2+}, Sr^{2+}, Hg^{2+}, Pb^{2+}, Cd^{2+}, Zn^{2+}, Co^{2+}, Ni^{2+}, Cu^{2+}, Fe^{3+} and Al^{3+}), only Al^{3+} exhibited an obvious emission change with a large Stoke's shift (a dramatic fluorescent enhancement at 585 nm was observed, $\Delta\lambda$= 345nm), whereas the remaining other ions had no significant response on the fluorescence emission spectra of **L1**. It strongly suggested that **L1** possessed a specific response towards Al^{3+} ions (Fig. 1a).

Fluorescence titration experiments were performed to investigate the detail complexation process of probe **L1** with Al^{3+} (Fig. 1b). In the absence of metal ions, probe **L1** only exhibited a weak excimer emission peak ($\lambda_{ex}/ \lambda_{em} =$ 240 nm/ 495 nm, the quantum yield Φ = 0.012 *versus* quinine sulfate as reference material, Φ = 0.56, Fig. S7a). This can be attributed to the tertiary *N* atom in the tren fragment of **L1**, which provides an unshared electron pair, and would quench the monomer and excimer emissions of the
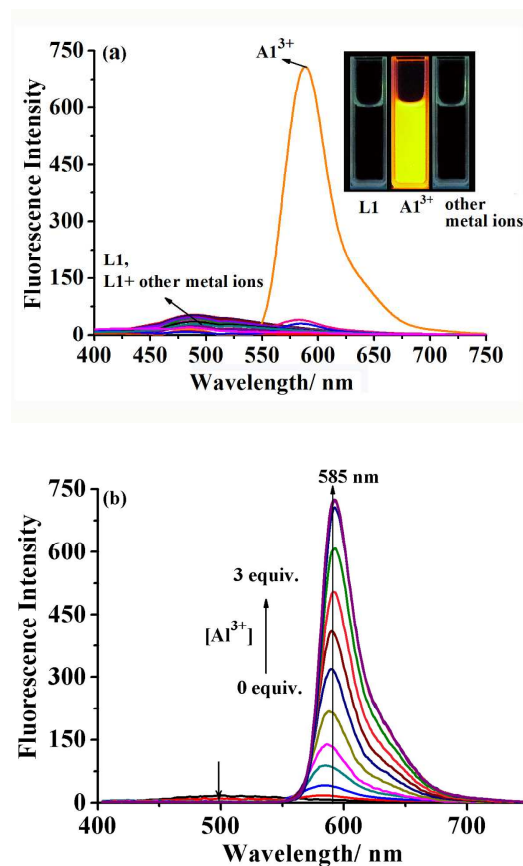
Figure 1. (a) Fluorescence spectra of probe **L1** (10 μM, pH 7, H_2O/CH_3CN, 2/98, v/v) with 20 equiv. of different metal ions (inset shows the colour change of probe **L1** in the absence and the presence of Al^{3+} under UV-vis light.); (b) Fluorescence spectral changes of probe **L1** (50 μM, pH 7, H_2O/CH_3CN, 2/98, v/v) solution upon addition of Al^{3+} (0 ~ 3 equiv.). $\lambda_{ex} / \lambda_{em}$ = 240 nm/ 585 nm.

naphthalene moiety by a PET process. Meanwhile, the rhodamine is present in its spirolactam state and suppresses the energy transfer from the excited naphthalene moiety to lactonized rhodamine.[13] Upon increasing the concentration of Al^{3+}, the naphthalene excimer emission maximum at 495 nm was completely quenched. At the same time, a typical Rhodamine emission band centered at 585 nm with a 32.5-fold enhancement was observed (Φ = 0.39) which suggested that an efficient FRET process takes place from the donor (naphthalene) group to the acceptor (Rhodamine) group. This could be attributed to the chelation of Al^{3+} with the oxygen, sulfur atoms and thiourea moiety resulting in inhibition of the PET process, whilst inducing the rhodamine spirolactam ring-opening of **L1**. Consequently, the increased overlap between the emission of the energy donor and absorption of the energy acceptor led to the intramolecular FRET (Fig. S8).[13] The FRET efficiency between the donor and acceptor moieties was calculated to be 71 % by the literature method[14]. The spectral changes were almost complete upon the addition of 2 equiv. of Al^{3+}, consistent with the molar ratio (Fig. S9a). The 1:2 **L1**·$2Al^{3+}$

ARTICLE

complex stoichiometry was further confirmed by a Job's plot (Fig. S9b).
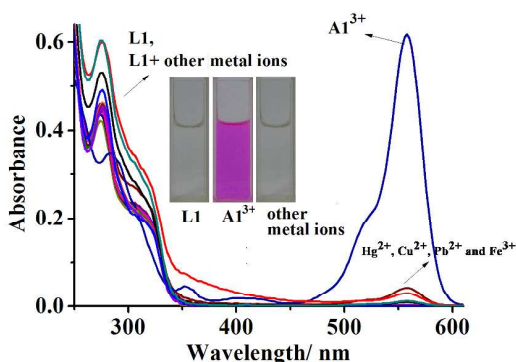
Figure 2. Absorption spectra of probe **L1** (10 μM, H₂O/CH₃CN, 2/98, v/v, pH 7) with 20 equiv. of different metal ions. Inset shows the colour change of probe **L1** in the absence and the presence of Al³⁺ under day light, λ_{max}=558 nm.

Similar selectively was also observed in the UV-vis absorption spectra (Fig. 2). Following the addition of 20 equiv. of various cations, only the addition of Al³⁺ resulted in an acute absorption band centered at 555 nm, which clearly indicated the complexation of Al³⁺ and the formation of a ring-opened structure for the rhodamine moiety. The visible colour change from colourless to pink also supported the tunable 'close-open' rhodamine spirolactam structure (Fig. 2 inset).[15] Furthermore, this remarkable colour change can be employed to conveniently distinguished Al³⁺ by the naked eye. Although there was a slight absorption at 558 nm in the presence of Hg²⁺, Cu²⁺, Pb²⁺ and Fe³⁺ ions, it did not create any significant interference for the detection of Al³⁺ (Fig. 3), which was consistent with the fluorescent result (Fig. S10).

UV-vis absorption titration experiments were also employed to investigate the binding process of **L1** towards Al³⁺. As shown in Figure S13a, a new absorption band at 558 nm, which gradually increased upon the addition of Al³⁺ was
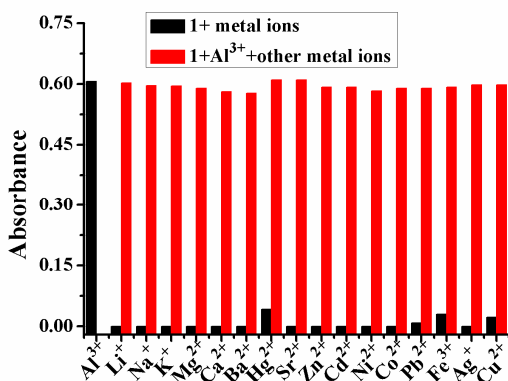
Figure 3. Absorption response of probe **L1** (10 μM, H₂O/CH₃CN, 2/98, v/v, pH 7). Black bars: the absorbance of probe **L1** at 558 nm on addition of the respective metal ions (20 equiv.). Red bars: the absorbance of **L1·2Al³⁺** complex at 558 nm on addition of the respective competing metal ions (20

equiv.). Metal ions including Al³⁺, Li⁺, Na⁺, K⁺, Mg²⁺, Ca²⁺, Ba²⁺, Sr²⁺, Hg²⁺, Pb²⁺, Cd²⁺, Zn²⁺, Co²⁺, Ni²⁺, Cu²⁺, Ag⁺ and Fe³⁺.

observed, and this reached equilibrium at 2 equiv. of Al³⁺ (Fig. S13b). This suggested a 1:2 binding ratio, which was further supported by a Job's plot analysis (Fig. S13c) for this complexation. These results are consistent with the fluorescent analysis results (Fig. S9). The 1:2 of **L1·2Al³⁺** complex was further confirmed by MALDI-TOF mass spectrometry. A mass peak at *m/z* 989.43021 (calculated value 989.39114) was observed which corresponded to [**L1** + 2Al -5 H]⁺, strongly suggestive of the formation of a 1:2 complex (Fig. S14).

The binding mode of **L1** with Al³⁺ was examined by ¹H NMR spectroscopy in CD₃CN/CDCl₃ (4/6, v/v). The partial ¹H NMR spectra of **L1** before and after treatment with various concentrations of Al(ClO₄)₃ are shown in Figure 4. The presence of Al³⁺ can affect the proton signals which are close to the Al³⁺ binding site. The ring protons signals of rhodamine was shifted downfield and became broaden and gradually disappeared upon addition of Al³⁺. This indicated the opening of the spirolactam ring upon coordination to Al³⁺ with associated charge transfer at the xanthene moiety. At the same time, the methylene protons of the tren moiety also shifted downfield, which strongly suggested that Al³⁺ was bound to the
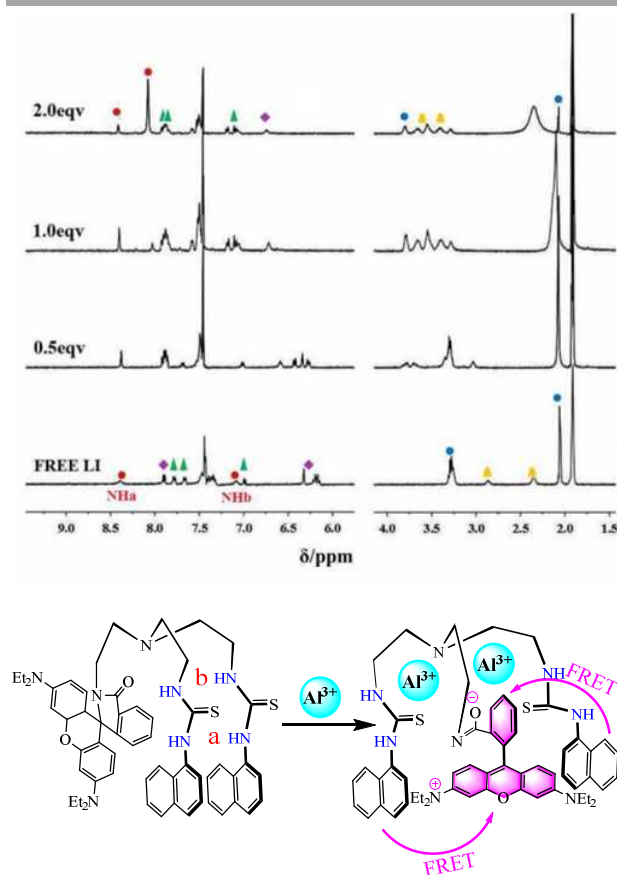
Figure 4. (up) Partial ¹H NMR spectra of probe **L1** (5 mM) and increasing concentrations of Al³⁺ in CD₃CN/CDCl₃(4/6) solution at

298K; (bottom) Possible binding model of the probe **L1** with Al^{3+} ion complexes.

nitrogen atoms of the tren. In addition, the aromatic protons of the naphthyl thiourea were only slightly shifted downfield ($\Delta\delta$ = 0.016–0.214 ppm, respectively) given the involvement of the thiourea sulfur atoms in the Al^{3+} binding process. The latter resulted in the decrease of electron density at these moieties which also resulted in the NH thiourea protons being shifted downfield ($\Delta\delta$ = 0.023 – 0.992 ppm, respectively). These observations suggested that the Al^{3+} was bound to probe **L1** through one oxygen atom of a carbonyl group, nitrogen atoms of tren and sulfur atoms of thiourea. Consequently, combined with the UV and fluorescence assay results, we proposed the possible binding model shown in Fig. 4 (bottom).

Recognition properties of probe L1 towards anions

Thiourea subunits are widely used in the design of neutral receptors for anions, owing to their ability to act as H-bonding donors.[16] Hence, we also investigated the sensing properties of **L1** towards different anions by fluorescence, absorption and ^1H NMR spectroscopy.

In 1,4-dioxane/water (v/v, 99/1) solution, probe **L1** (10 µM, Fig. 5a) exhibited absorption peaks at 274 nm and 310 nm, which correspond to the $\pi \to \pi^*$ and $n \to \pi^*$ transitions of the naphthalene groups, respectively.[12] Upon the addition of 20 equiv. of various anions, *viz.* F^-, Cl^-, Br^-, NO_3^-, $H_2PO_4^-$, HSO_4^-, ClO_4^-, AcO^- and PF_6^-, there were no detectable changes, except in the case of I^-, which indicated the high selectivity of **L1** for I^- anions. Two new absorption peaks at 295 nm and 360 nm appeared in the presence of

20 equiv. of I^- ions, which suggested the formation of an **L1**·I complex. Furthermore, UV titration experiments revealed the details of the complexation process; the new absorption peaks at 295 nm and 360 nm gradually enhanced upon increasing the amount of I^- (Fig. S17). However, no detectable absorption for the rhodamine moiety (*e.g.* absorption band at 558 nm) was observed, which indicated the rhodamine moiety did not contribute to the complexation process. Moreover, the characteristic absorptions for the naphthalene group (274 nm and 310 nm) were unchanged. Consequently, we speculate that the new absorption peaks at 295 nm and 360 nm can be attributed to the formation of a new intramolecular hydrogen bond, leading to the formation of two six-membered rings via hydrogen bonding with the I^- anion (Fig. 5d).

We then further employed the fluorescent method to analyze the recognition properties of probe **L1** towards anions. Similar selectivity was observed by using fluorescent analysis, namely probe **L1** exhibited a high selectivity for I^- as evidenced by a fluorescence decrease (Fig. 5b). According to the fluorescent titration experiments, only the excimer emission was observed, *ie* no detectable monomer emission can be observed (Fig. S19). This indicated the formation of hydrogen-bonding between the I^- ion and the NH of the two thiourea moieties and diminished the π-π stacking interaction between the two naphthalenes.

In order to confirm our speculation and to obtain additional information about the coordination mode of **L1** with I^-, ^1H NMR titration experiments was performed in $CDCl_3$ (Fig. 5c). Both the N*Ha* and N*Hb* protons were shifted downfield ($\Delta\delta$ 0.153 ppm and 0.065 ppm, respectively) upon the addition of 3.0 equiv. of I^-, which strongly suggested that the thiourea N*H* protons were
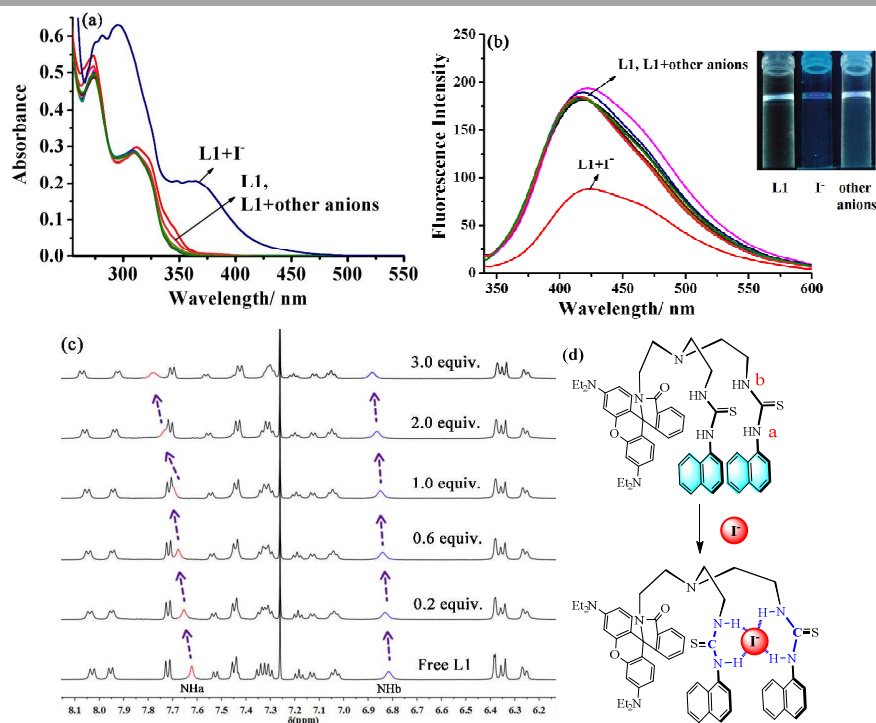
Figure 5. Absorption (a) and fluorescence (b) spectra of probe **L1** (10 µM, 1,4-Dioxane/H_2O, v/v, 99/1) with different anions (200 µM). Anions: I^-,

F^-, Cl^-, Br^-, NO_3^-, $H_2PO_4^-$, HSO_4^-, ClO_4^-, A_CO^-, PF_6^-. λ_{ex} = 310 nm; (c) Partial ^1H NMR spectra of probe **L1** (5 mM) and increasing concentrations of I^- in $CDCl_3$ solution at 298K; (d) proposed binding model of the probe **L1** with I^- ion complexes.

Table 1 Analysis parameters for **L1** and detection of Al^{3+} and I^-.

Method		The linear range of the calibration curve (μM)	Correlation coefficient	LOD ($\times 10^{-8}$ M)	Association constants K_a
Fluorescence	Al^{3+}	16.7 ~ 95	0.9935	6.2	K_1 = 777.45 (±0.391) M^{-1} K_2 = 3.099×10^5 (±0.391) M^{-1} R = 0.9898
	I^-	1 ~ 500	0.9953	9.2	K_a = 1.04×10^4 (±0.033) M^{-1} R = 0.9910
Absorption	Al^{3+}	10.5 ~ 95	0.9055	580	K_1 = 1225.8 (±0.312) M^{-1} K_2 = 2.654×10^5(±0.312) M^{-1} R = 0.9842
	I^-	2.0 ~ 480	0.9578	42	K_a = 2.08×10^5 (±0.005)M^{-1} R = 0.9975

interacting with I^-. Furthermore, the doublet signals of the naphthyl ring were also shifted slightly downfield. These observations suggested that the complexation between **L1** and the I^- anion occurs via multiple hydrogen bonding. Additionally, both the UV spectra and the fluorescence Job's plot analysis revealed a 1:1 stoichiometry (Fig. S18 & S20). Consequently, we proposed the possible binding mode as shown in Figure 5d, where the I^- ion was fixed in the middle of two 1-naphthyl isothiocyanate moieties through hydrogen bonds which diminished the π-π stacking interaction between the two naphthalenes and resulted in the observed decreased fluorescence.

To further investigate the practical applicability of probe **L1** (10 μM) as an I^- ion selective fluorescent probe, competitive anion experiments were carried out in the presence of I^- mixed

Figure 6. Fluorescence images of PC3 cells: (a) bright-field image of cells after incubation with probe **L1** (20 μM); (b) fluorescence image of (a) in red or green channel; (c) fluorescence images of PC3 cells incubated with probe

L1 (20 μM) for 40 min, then treated with Al^{3+} (100 μM) for 40 min in the red channel; (d) fluorescence images of (c) in green channel; red channel: λ_{ex} = 510 nm ~ 550 nm; green channel: λ_{ex} = 450 nm ~ 490 nm.

with 50 equiv. of the coexisting anions F^-, Cl^-, Br^-, I^-, HSO_4^-, NO_3^-, ClO_4^-, PF_6^-, AcO^- and $H_2PO_4^-$ in 1,4-dioxane/water (v/v, 99/1) solution. As shown in Fig. S21, no interference in the detection of I^- with probe **L1** was observed in the presence of these other competitive anions. Accordingly, these observations strongly suggested that probe **L1** can serve as a selective probe for I^- in the presence of the above mentioned ions for real life applications.

The detection of linear relationships and limits of detection (LOD = 3σ /slope) for probe **L1** with Al^{3+} and I^-, under the optimal conditions, are summarized in Table 1 (Figs. S11 ~ S12, S15 ~ S16 & S22 ~ S25). A relatively wide linear range can be calculated which will allow for more convenient/widespread detection applications. The LOD of probe **L1** towards the cation Al^{3+}, and the anion I^- was of the order of 10^{-8} M by fluorescence or 10^{-6} M by the colorimetric method, which is far below most previously reported systems (Table S1).[17] This data strongly suggests that the probe **L1** is a sensitive dual function sensor for the detection of Al^{3+} and I^-.

Cell imaging study

The capability of probe **L1** to detect Al^{3+} within living cells was investigated by fluorescence imaging on a fluorescent inverted microscope. The prostate cancer (PC3) cells were incubated with probe **L1** (20 μM) in RPMI medium for 40 min at 37 °C and washed with fresh RPMI medium to remove any excess of probe **L1**. No intracellular fluorescence was monitored in the bright-field image (Fig. 6a) and in the fluorescence image (Fig. 6b). The incubated cells were then further treated with 100 μM of Al^{3+} for 40 min, and a dramatic intracellular fluorescence was observed (Fig. 6c and Fig. 6d). It unambiguously confirmed that the red or green fluorescence was induced by the response of probe **L1** towards the
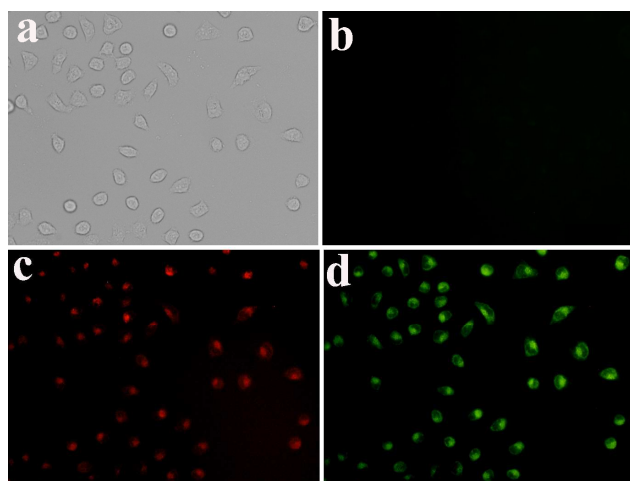
intracellular Al^{3+} ions. The strong red or green fluorescence emission indicated a high permeability of probe **L1** into living cells, which can be applied for the monitoring of intracellular Al^{3+} in PC3 cells by *in vitro* imaging and also potentially by *in vivo* methods.

Conclusions

In summary, rhodamine B and 1-naphthaleneisothiocyanate were employed here to construct the tripodal probe **L1**, which possessed the capability for forming a FRET probe due to fluorescent spectra overlap. The recognition properties of probe **L1** were fully investigated by fluorescence, absorption and ^{1}H NMR spectroscopic titration and mass spectrometry. For the cation recognition study, probe **L1** exhibited high sensitivity and selectivity towards Al^{3+} through a "FRET" fluorescence response with a large Stoke's shift and colorimetric response with low detection limits of 7.3×10^{-8} M. On the other hand, the anion recognition study revealed that probe **L1** also possessed high sensitivity (4.6×10^{-7} M) and selectivity towards I^- observed via a decrease in fluorescence. This is a significant addition to the number of detection assays available for I^-, particularly as there are comparatively few selective fluorescent probes for I^-. Additionally, probe **L1** has been exploited for the detection of Al^{3+} in living cells. The successful fluorescence imaging experiments suggested that probe **L1** possessed good permeability into living cells, which can be applied for monitoring intracellular Al^{3+} in PC3 cells by *in vitro* imaging and also potentially by *in vivo* methods. This work provides a promising strategy for the detection of metal ions and anionic species in biological and environmentally relevant systems.

Experimental

Materials and methods

Unless otherwise stated, all reagents used were purchased from commercial sources and were used without further purification. The solutions of the metal ions were prepared from their nitrate salts (Aldrich and Alfa Aesar Chemical Co., Ltd.). All the anions used were tetra-*n*-butylammonium salts (Sigma-Aldrich Chemical Co.), and were stored in a desiccator under vacuum containing self-indicating silica. Other chemicals used in this work were of analytical grade and were used without further purification. Double distilled water was used throughout. Fluorescence spectral measurements were performed on a Cary Eclipse fluorescence spectrophotometer (Varian) equipped with a xenon discharge lamp using a 1 cm quartz cell. UV-Vis absorption spectra were recorded on a UV-1800 spectrophotometer (Shimadzu) in a 1 cm quartz cell. IR spectra were obtained using a Vertex 70 FT-IR spectrometer (Bruker). ^{1}H and ^{13}C NMR spectra were measured on a JEOL JNM-ECZ400S 400 MHz NMR spectrometer (JEOL) and a WNMR-I 500 MHz NMR spectrometer (Wuhan Institute of Physics and Mathematics, Chinese Academy of Sciences) respectively at room temperature using TMS as an internal standard. ESI-MS

spectra were recorded on a Q Exactive spectrometer (Thermo). MALDI-TOF mass spectra were measured on a BIFLEX III ultra-high resolution Fourier transform ion cyclotron resonance (FT-ICR) mass spectrometer (Bruker) with α-cyano-4-hydroxycinnamic acid as matrix. Microelectrode layers using the sputtering and lift-off process with the standard photo-lithography (EVG 610, Austria). Cell fluorescence imaging was performed using an Ti (Nikon) fluorescent inverted phase contrast microscope.

Syntheses

Synthetic of intermediate 1

A mixture of tris(2-aminoethyl)amine (4.0 g, 27.36 mmol), Rhodamine B (1.638 g, 3.42 mmol) in dry ethanol (60 mL) was refluxed for 24 h under N_2 atmosphere. The solvent was removed by evaporation. The residue was extracted with CH_2Cl_2 (100 mL) three times, washed with water and dried with $MgSO_4$ overnight. The CH_2Cl_2 solvent was removed by evaporation and gave a light red oil product. The crude product was purified by column chromatography (MeOH/CHCl$_3$/NEt$_3$ = 9/1/1，v/v) to give 1.71g colourless oil pure product **1** in 87.3% yield. ^{1}H NMR (500 MHz, CDCl$_3$) δ ppm 7.89(d, J = 5.0 Hz, 1H, ArH), 7.44-7.46 (br, 2H, Ar*H*), 7.10 (bs, 1H, Ar*H*), 6.40 ~ 6.42 (m, 4H, Ar*H*), 6.27 (d, J = 5.0 Hz , 2H, Ar*H*), 3.34 (q, J = 10.0 Hz, 8H, NC*H*$_2$CH$_3$), 3.15 (m, 2H, NC*H*$_2$CH$_2$N), 2.55-2.57 (m, 4H, NC*H*$_2$CH$_2$N), 2.36 (t, J = 5.0 Hz, 4H, NC*H*$_2$CH$_2$N), 2.24 (t, J = 5.0 Hz, 4H, NC*H*$_2$CH$_2$N), 1.17 (t, J = 10.0 Hz, 12H, NCH$_2$C*H*$_3$); ^{13}C NMR (125 MHz, CDCl$_3$) δ 12.16, 37.51, 38.54, 43.96, 51.29, 54.79, 56.91, 97.23, 104.97, 107.71, 122.25, 123.43, 127.79, 128.47, 131.08, 132.03, 148.41, 152.55, 153.11, 167.41ppm.

Synthetic of probe L1

A mixture of intermediate **1** (1.16 g, 2.03 mmol) and 1-naphthyl isothiocyanate (740 mg, 4.00 mmol) in dry CHCl$_3$ (120 mL) was refluxed overnight under N_2 atmosphere. The solvent was removed by evaporation. The residue was extracted with CH_2Cl_2 (100 mL) three times, washed with water and dried with $MgSO_4$ over night. The CH_2Cl_2 solvent was removed by evaporation. The crude product was purified by column chromatography (EtOAc/Hexane = 7/3, v/v) to give 1.45 g of white solid **L1** in 76.3% yield. m.p. 125 ~127 °C; IR (KBr, vcm^{-1}): 3333 (N-H), 1603 (C=C), 1518 (C-N-H), 1103 (C-O), 772(Ar-H), 625(Ar-H). ^{1}H NMR (500 MHz, CDCl$_3$) δ: 8.13(s, 2 H, CS*NH*), 7.92 (d, J = 8.0Hz, 2 H, Ar*H*), 7.79 (d, J = 8.0 Hz, 2 H, Ar*H*), 7.67 (d, J = 8.0 Hz, 2 H, Ar*H*), 7.61(d, J = 8.0Hz, 2 H, Ar*H*),7.27 ~ 7.48 (m, 9 H, Ar*H*), 7.12 ~ 7.24 (s, 2 H, CS*NH*), 7.09 (d, J = 8.0 Hz, 2 H, Ar*H*), 6.38(d, J = 4.0Hz,2H, Ar*H*), 6.21-6.27(m, 4H, Ar*H*), 3.25 ~ 3.41 (m, 12 H, NC*H*$_2$CH$_3$), 2.84 ~ 2.87 (t, 2 H, NC*H*$_2$CH$_2$N), 2.35 ~ 2.39 (t, 4 H, NC*H*$_2$CH$_2$N), 1.92 ~ 1.94 (t, 2H,N 2 H, NC*H*$_2$CH$_2$N), 1.07-1.18 (m, 12 H, NCH$_2$C*H*$_3$); ^{13}C NMR (500 MHz, CDCl$_3$) δ 12.56, 37.72, 40.24, 44.41, 53.55, 54.33, 66.81, 97.67, 104.66, 108.48, 118.01, 121.10, 122.68, 123.18, 124.08, 125.49, 125.58, 126.07, 126.63, 128.38, 128.44, 128.70, 131.02, 133.00, 134.09, 134.52, 149.03, 152.86, 153.62, 156.62, 169.55 ppm;

ARTICLE

MS (MALDI-TOF) Calcd for $[C_{56}H_{60}N_8O_2S_2]$: m/z 940.42806, Found: m/z 941.17524 $[M+H]^+$.

Spectral measurement

To a 10 mL volumetric flask containing different amounts of ions, the appropriate amounts of the solution of probe **L1** were added using a micropipette. For Al^{3+}, the system was then diluted with CH_3CN/H_2O (49/1, v/v) mixed solvent to 10 mL; for I^-, it was diluted with 1,4-dioxane/water (v/v,99/1) to 10 mL, and then the fluorescence and absorption sensing of the ions was conducted. The fluorescence and UV-vis spectra were measured after addition of the ions at room temperature and when equilibrium was reached. Fluorescence measurements were carried out with an excitation and emission slit width of 10 nm.

Cell culture and fluorescence imaging

PC3 cells were grown using a Roswell Park Memorial Institute Medium Modified supplemented with 10% fetal bovine serum, 100 U/mL penicillin and 100 μg/mL streptomycin at 37 °C and 5% CO_2. One day prior to imaging, the cells were seeded in 6-well flat-bottomed plates. The next day, the cells were incubated with 20 μM of probe **L1** for 40 min at 37 °C. Before incubating with 100 μM $Al(ClO_4)_3$ for another 40 min, the cells were rinsed with fresh culture medium three times to remove the remaining sensor, then the fluorescence imaging of intracellular Al^{3+} was observed under an inverted fluorescence microscope excited with UV light.

Conflicts of interest

There are no conflicts of interest to declare.

Acknowledgements

Notes and references

1   (a) A. Sahana, A. Banerjee, S. Lohar, A. Banik, S. K. Mukhopadhyay, D. A. Safin, M. G. Babashkina, M. Bolte, Y. Garcia, D. Das, *Dalton Trans*., 2013, **42**, 13311-13314. (b) D. Maity, T. Govindaraju, *Chem. Commun*., 2010, **46**, 4499-4501.

2   (a) W. S. Miller, L. Zhuang, J. Bottema, A. J. Wittebrood, P. D. Smet, A. Haszler and A. Vieregge, *Mater. Sci. Eng. A*., 2000, **280**, 37-49. (b) G. Ciardelli, N. Ranieri, *Water Res*.,
2001, **35**, 567-572. (c) R. A. Yokel, C. L. Hicks and R. L. Florence, *Food Chem. Toxicol*., 2008, **46**, 2261-2266.

3   D. Sarkar, P. Ghosh, S. Gharami, T. K. Mondal and N. Murmu, *Sensor. Actuators B: Chem*., 2017, **242**, 338-346.

4   (a) B. Liu, P. F. Wang, J. Chai, X. Q. Hu, T. Gao, J. B. Chao, T. G. Chen and B. S. Yang, *Spectrochim. Acta A*., 2016, **168**, 98-103. (b) N. Chatterjee, S. B. Maity, A. Samadder, P. Mukherjee, A. R. Khuda-Bukhsh and P. K. Bharadwaj, *RSC Adv*.,. 2016, **6**, 17995-18001. (c) L. K. Kumawat, N. Mergu, M. Asif, V. K. Gupta, *Sensor. Actuators B: Chem*., 2016, **231**, 847-859. (d) Z. C. Liao, Z. Y. Yang, Y. Li, B. D. Wang and Q. X. Zhou, *Dyes Pigm*.,. 2013, **97**, 124-128.

5   S. Venturi, *Curr. Chem. Biol*., 2011, **5**, 155-167.

6   A. S. Green and E. Pearce, *Nat. Rev. Endocrinol*., 2012, **8**, 650-658.

7   S. Venturi, F. M. Donati, M. Venturi, A. Venturi, L. Grossi and A. Guidi, *Adv. Clin. Pathol*., 2000, **4**, 11-17.

8   C. P. Shelor and P. K. Dasgupta, *Anal Chim Acta*., 2011, **702**, 16-36.

9   S. Sandhu, R. Kumar, P. Singh, A. Walia, V. Vanita and S. Kumar, *Org Biomol Chem*., 2016, **14**, 3536-3543.

10 (a) W. Sun, S. G. Guo, C. Hu, J. L. Fan and X. J. Peng, *Chem. Rev*., 2016, **116**, 7768-7817; (b) E. Karakus, M. Ucuncu and M. Emrullahoglu, *Anal. Chem.*, 2016, **88**, 1039-1043; (c) S. Samanta, B. K. Datta, M. Boral, A. Nandan and G. Das, *Analyst*, 2016, **141**, 4388-4393; (d) H. Sui, Y. Wang, Z. Yu, Q. Cong, X. X. Han and B. Zhao, *Talanta*, 2016, **159**, 208-214; (e) Y. J. Chen, S. C. Yang, C. C. Tsai, K. C. Chang, W. H. Chuang, W. L. Chu, V. Kovalev and W. S. Chung, *Chem. Asian J.*, 2015, **10**, 1025-1034.

11 S. K. Kim and J. L. Sessler, *Chem. Soc. Rev*., 2010, **39**, 3784-3809.

12 C. Kaewtong, B. Pulpoka and T. Tuntulani, *Dyes and Pigments*., 2015, **123**, 204-211.

13 (a)C. Y. Li, Y. Zhou, Y. F. Li, X. F Kong, C. X. Zou and C. Weng, *Anal Chim Acta.,* 2013, **774**, 79-84.(b) Min Hee Lee, Hyun Jung Kim, Sangwoon Yoon, Noejung Park, and Jong Seung Kim. *Org. Lett.* **2008**, *10*, 213-216.(c) A. B. Othman, J. W. Lee, J. S. Wu, J. S. Kim, R. Abidi, P. Thuéry, J. Marc Strub, A. V. Dorsselaer and Jacques Vicens, *J. Org. Che.,* 2007, **72**, 7634-7640.

14 (a) G. W. Gordon, G. Berry, X. H. Liang, B. Levine and B. Herman, *Biophysical Journal*., 1998, **74**, 2702-2713. (b) M. H. Lee, D. T. Quang, H. S. Jung, J. Y. Yoon, C. H. Lee, J. S. Kim, *J. Org. Chem*., 72, 2007, 4242-4245.

15 (a) H. Kim, S. Lee, J. Lee and J. Tae, *Org. Lett*., 2010, **12**, 5342-5345; (b) X. C. Wang, J. Tao, X. Q. Chen and H. Yang, *Sensor. Actuators B: Chem*., **224**, 2017, 709-716; (c) K. B. Li, H. Wang, Y. Zang, X. P. He, J. Li, G. R. Chen and H. Tian, *ACS Appl. Mater. Interfaces*., **6**, 2014, 19600-19605.

16 (a) P. A. Gale, *Coord. Chem. Rev*., 2001, **213**, 79-128; (b) P. D. Beer and P. A. Gale, *Angew. Chem*., 2001, **40**, 486-516.

17 (a)S. Erdemir, M. Yuksekogul, S. Karakurt, O. Kocyigit, *Sensor. Actuators B: Chem*., 2017, **241**, 230-238. (b) Y. Long, J. Zhou, M. Yang, X. J. Liu, M. Zhang, B. Q. Yang, *Sensor and Actuators B*., 2016, **232**, 327-335. (C) J. Liu, Y. Qian, *Dyes and Pigments*., 2017, **136**, 782-790.

A bi-functional probe **L1** can high selectivity and sensitivity recognize Al^{3+} and I^- in practical sample even in living cell.
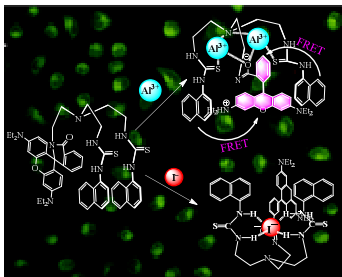
Electronic Supplementary Information (ESI)

Highly Selective Recognition of Al^{3+} and I^- ions using a Bi-functional

Fluorescent Probe

Zhao Li,[‡][a] Jiang-Lin Zhao,[‡][b] Yu-Tian Wu,[a] Lan Mu,[a] Xi Zeng,*[a] Zongwen Jin,*[b] Gang Wei,*[c] Ning Xie[e] and Carl Redshaw[d]

[a] *Key Laboratory of Macrocyclic and Supramolecular Chemistry of Guizhou Province, Guizhou University, Guiyang 550025, P.R. China*

[b] *Shenzhen Institutes of Advanced Technology, Chinese Academy of Sciences, 1068 Xueyuan Avenue, Shenzhen 518055, China.*

[c] *CSIRO Manufacturing, PO Box 218, NSW 2070, Australia*

[d] *Department of Chemistry, School of Mathematics & Physical Sciences, University of Hull, Hull HU6 7RX, U.K.*

[e] *College of Life Science, Shenzhen Key Laboratory of Microbial Genetic Engineering, Shenzhen University, Shenzhen 518060, China*

[‡] *Zhao Li and Jiang-Lin Zhao contributed equally to this work.*
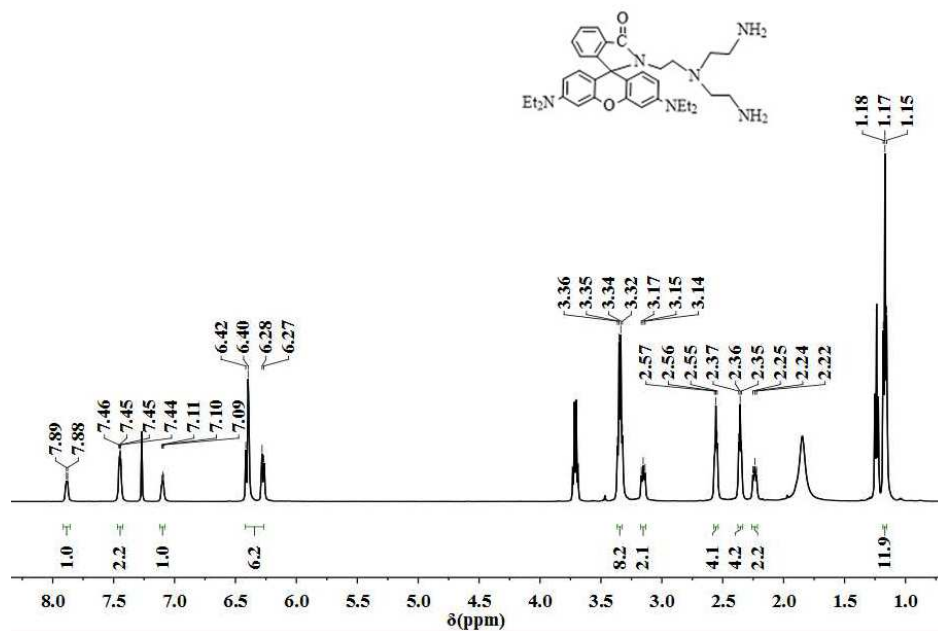
Figure S1. ^{1}H NMR spectrum of intermediate **1** (500 MHz, CDCl$_3$, 293 K).
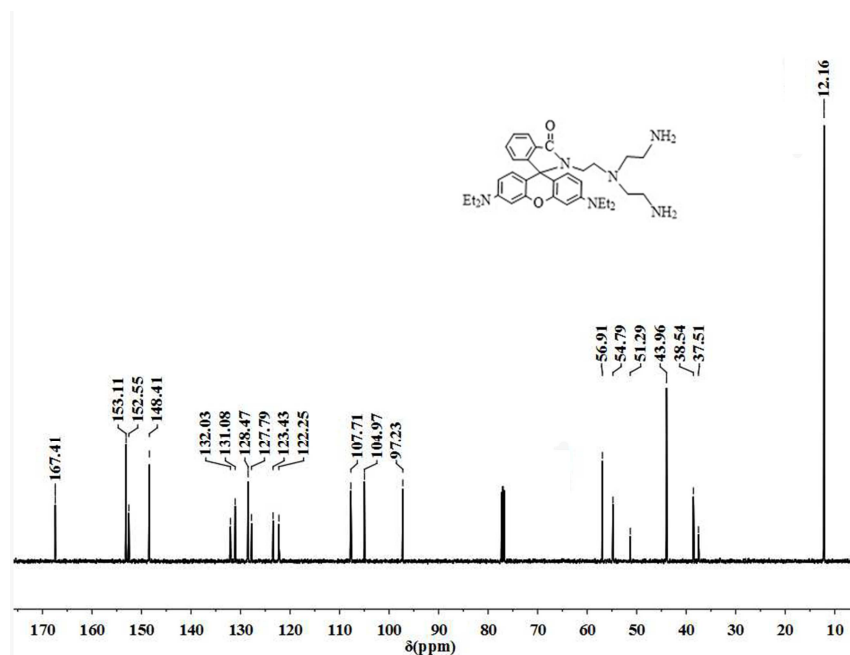
Figure S2. ^{13}C NMR spectrum of intermediate **1** (125 MHz, CDCl$_3$, 293 K).
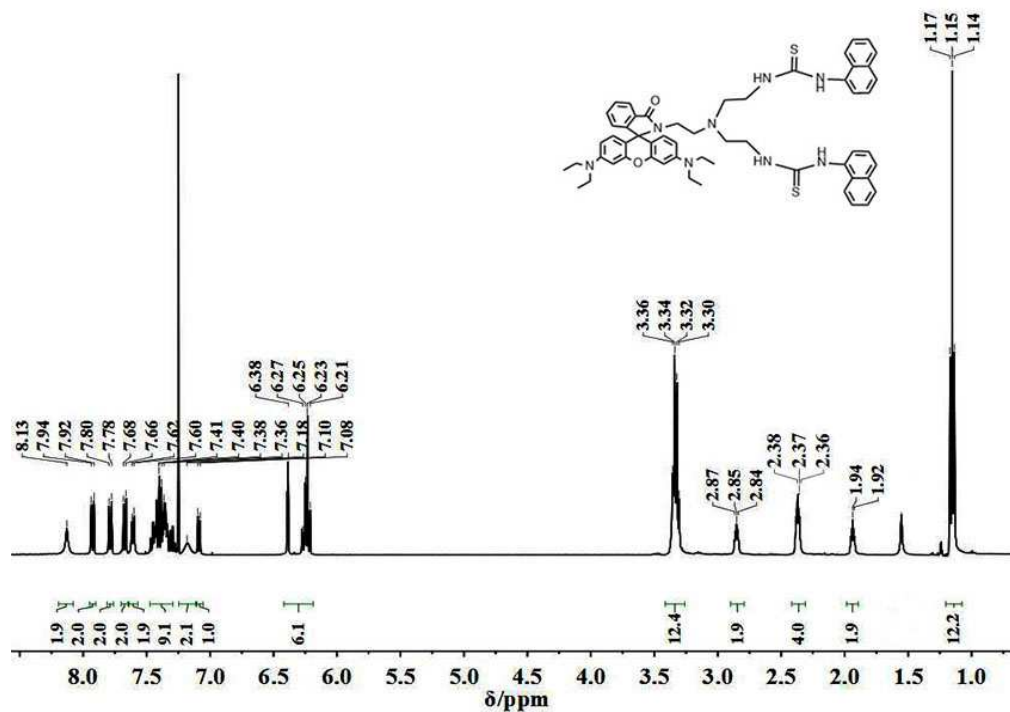
Figure S3. ^{1}H NMR spectrum of probe **L1** (500 MHz, CDCl$_3$, 293 K).
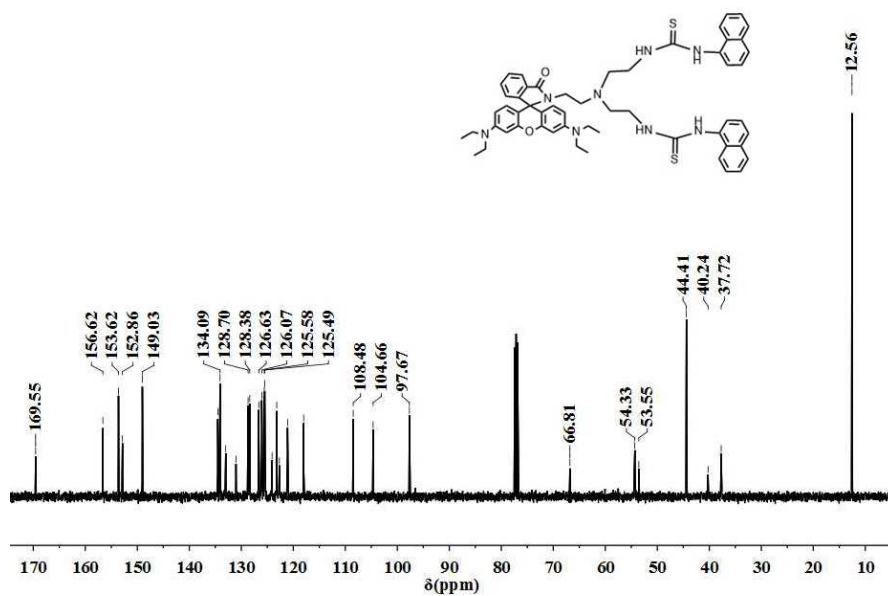
Figure S4. ^{13}C NMR spectrum of probe **L1** (125 MHz, CDCl$_3$, 293 K).
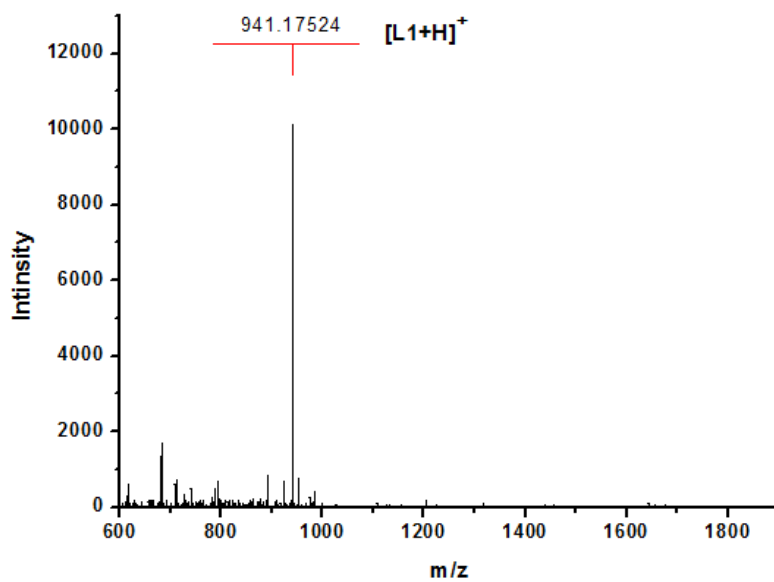
Figure S5. MALDI-TOF-MS spectrum of probe **L1**.
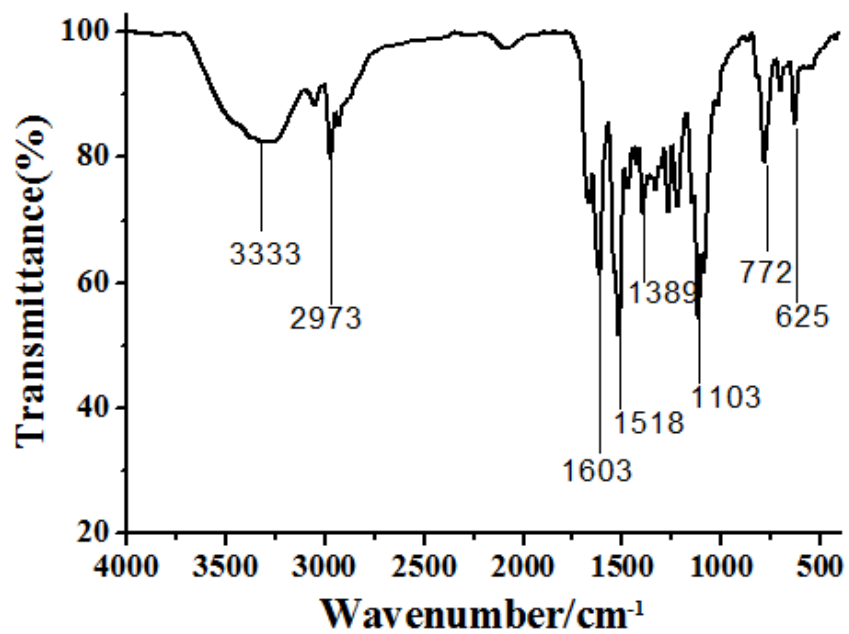
Figure S6. FT-IR spectrum of probe **L1**.
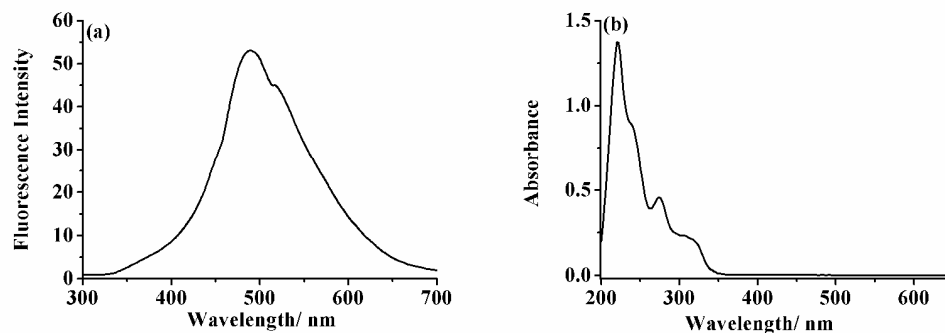
Figure S7. (a) Fluorescence spectra of probe **L1**; (b) Absorption spectra of probe **L1** (10 μM, H$_2$O/CH$_3$CN, 2/98, v/v, pH 7).
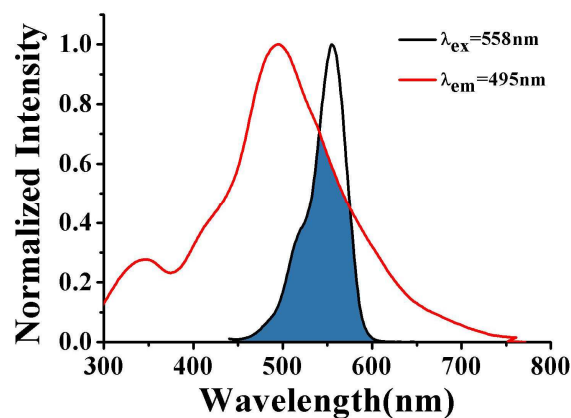
Figure S8. Spectral overlap between the energy donor naphthaline emission (black) and acceptor rhodamine absorption (red).
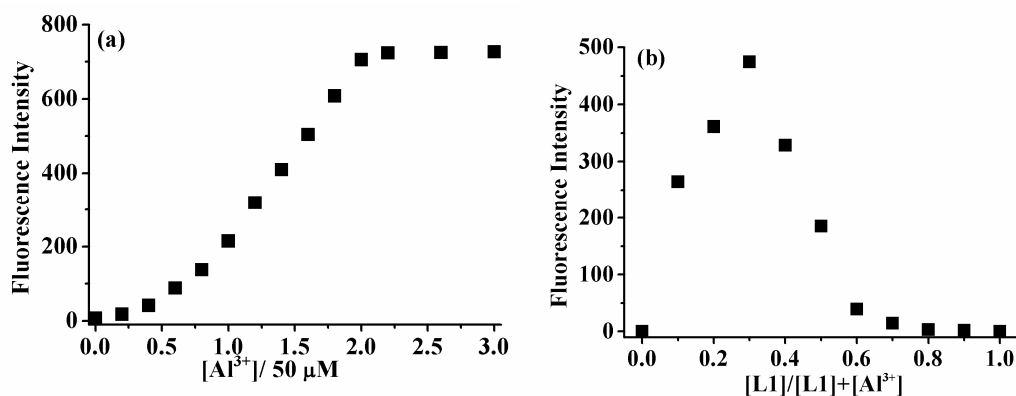
Figure S9. The plot of fluorescence intensity of probe **L1** as a function of Al^{3+} concentration (a) and the Job's plot data (b).
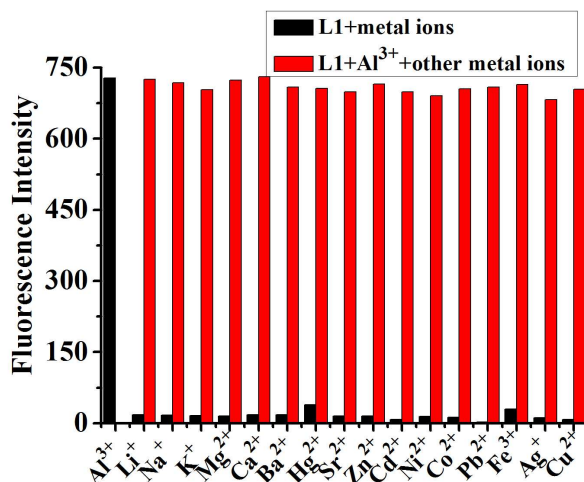
Figure S10. Fluorescence response of probe **L1** (10 μM, H_2O/CH_3CN, 2/98, v/v, pH 7). Black bars: emission intensity of probe **L1** at 585 nm with the addition of the respective metal ions (20 equiv.). Red bars: emission intensity of **L1·2Al^{3+}** complex at 585 nm with the addition of the respective competing ions (20 equiv.). Metal ions including Al^{3+}, Li^+, Na^+, K^+, Mg^{2+}, Ca^{2+}, Ba^{2+}, Sr^{2+}, Hg^{2+}, Pb^{2+}, Cd^{2+}, Zn^{2+}, Co^{2+}, Ni^{2+}, Cu^{2+}, Ag^+ and Fe^{3+}, $\lambda_{ex} = 240$ nm.
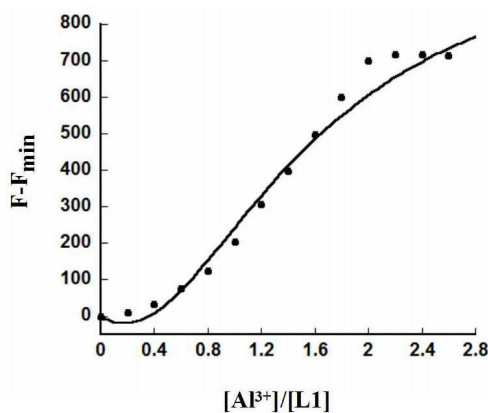
Figure S11. Non-linear plot of probe **L1** (50 μM) assuming a 1:2 stoichiometry for association between probe **L1** and Al^{3+} in CH_3CN/H_2O (v/v, 98/2, pH 7) solution by fluorescence spectroscopy; $\lambda_{ex}/\lambda_{em} = 240$ nm/585 nm.[1]

The fluorescence spectrum association constants of Al^{3+} were calculated by nonlinear fitting using the following formula [Eq. (1)]:

$$\Delta F_{Al} = \frac{\kappa_{\Delta HG}[H_0] + \kappa_{\Delta HG\,2}[H_0]K_1K_2[G]^2}{1 + K_1[G] + K_1K_2[G]^2} \tag{1}$$

where ΔF_{Al} is the change in the fluorescence intensity of the **L1** upon gradual addition

of the Al^{3+}, $\kappa_{\Delta HG}$ refers to the different proportionality constant of the complex HG

and the free host, and $\kappa_{\Delta HG_2}$ refers to the different proportionality constant of the

complex HG_2 and the free host. The total concentrations of host and guest are denoted by [H] and [G], respectively.

Equation(1) is noting also the relevant mass balance eqn (2), molar concentration of the 1 : 1 complex are denoted by [HG], [HG2] refers to 1 : 2 complex[1].

$$[H0] = [H] + [HG] + [HG2] \tag{2}$$

$R = 0.9898$, $K_1 = 777.45\ (\pm 0.391)\ M^{-1}$, $K_2 = 3.099 \times 10^5\ (\ \pm 0.391)\ M^{-2}$.

Reference:

[1] P. Thordarson, *Chem. Soc. Rev.*, 2011, **40**, 1305-1323.
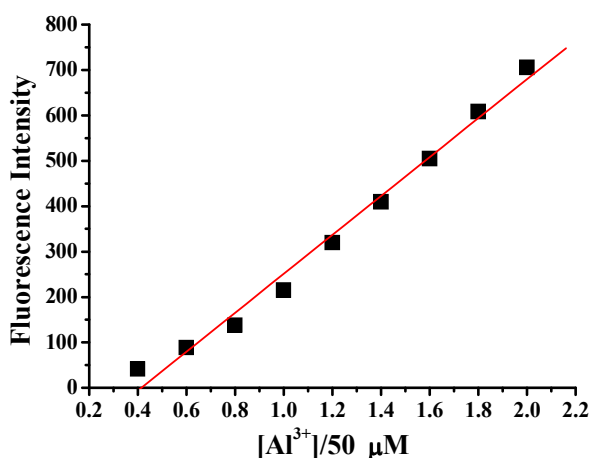
Figure S12. Fluorescence intensity calibration curve of probe **L1** (50 μM) as a function of Al^{3+} concentration in CH_3CN/H_2O (v/v, 98/2, pH 7) solution; $\lambda_{ex}/\lambda_{em} =$ 240 nm/585 nm. Y = 428.8 X - 177.8, R = 0.9935, LOD = 0.062 μM.
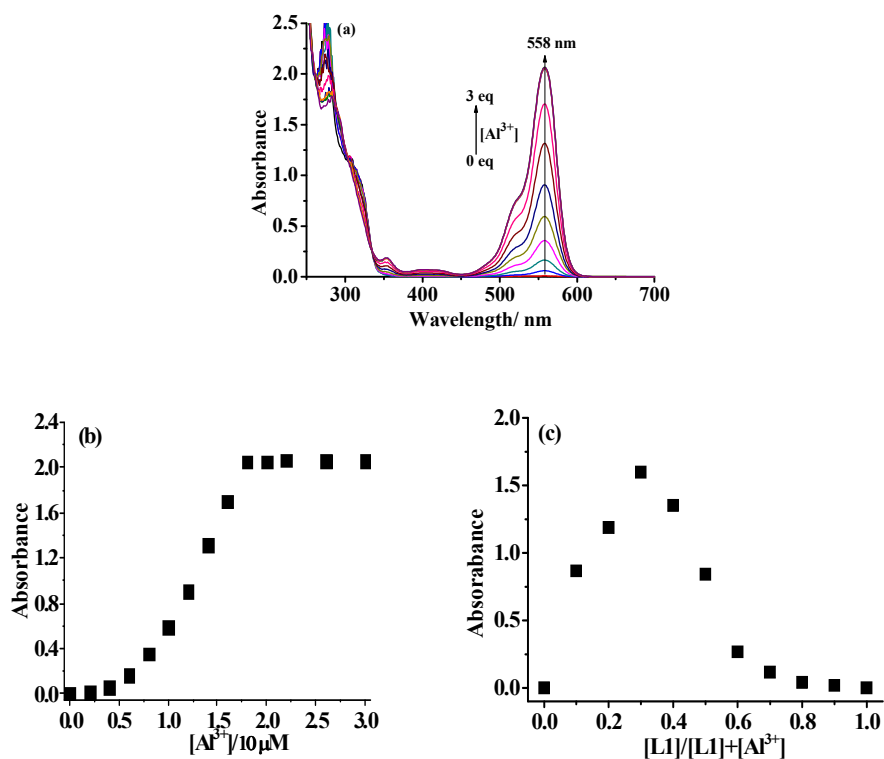
Figure S13. (a)Absorption spectral changes of probe **L1** (pH 7, 50 μM, H$_2$O/CH$_3$CN, 2/98, v/v) solution upon addition of Al^{3+} (0 ~ 30 μM); (b) the plot of absorbance at 558nm of probe **L1** as a function of Al^{3+} concentration and (c) the Job's plot data.
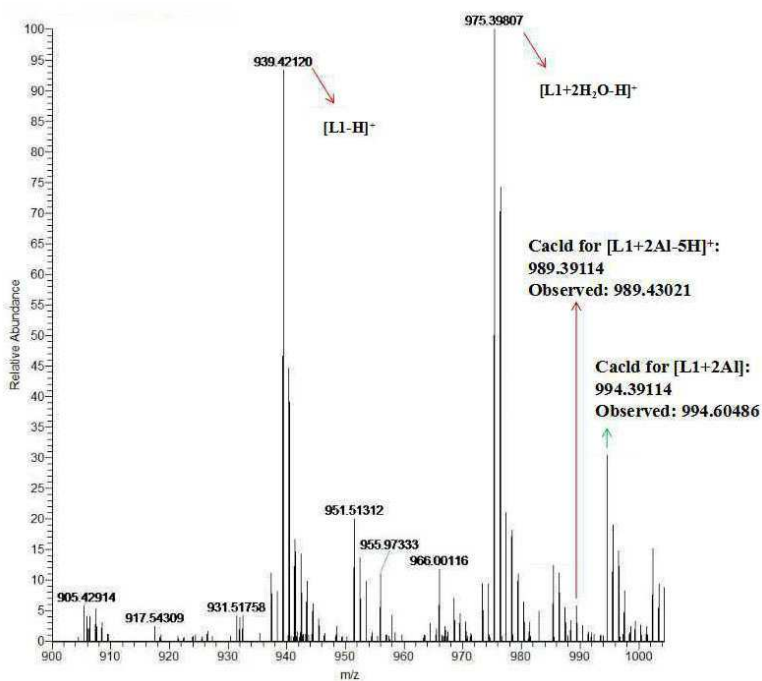
Figure S14. MALDI-TOF-MS spectrum of **L1·2Al** complex.
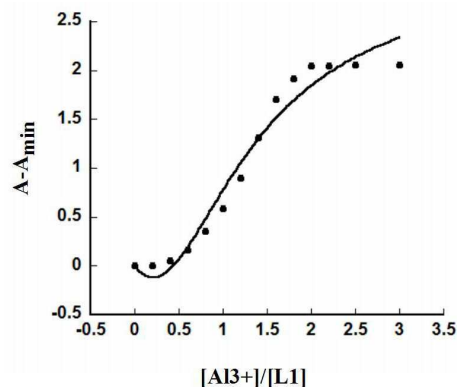
Figure S15. Non-linear plot of probe **L1** (50 μM) assuming a 1:2 stoichiometry for association between probe **L1** and Al^{3+} in CH_3CN/H_2O (v/v, 98/2, pH 7) solution by absorption spectroscopy. $\lambda_{max} = 558$ nm.[1]

The UV spectrum association constants of Al^{3+} were calculated by nonlinear fitting using the following formula [Eq. (3)]:

$$\Delta A_{Al} = \frac{\varepsilon_{\Delta HG}[H_0]K_1[G] + \varepsilon_{\Delta HG\,2}[H_0]K_1K_2[G]^2}{1 + K_1[G] + K_1K_2[G]^2} \tag{3}$$

where ΔA_{Al} is the change in the UV absorption intensity of the **L1** upon gradual addition of the Al^{3+}, and $\varepsilon_{\Delta HG}$ refers to the different molar absorptivity of the free host and the complex of one host and one guest, $\varepsilon_{\Delta HG\,2}$ refers to the different molar absorptivity of the free host and the complex of one host and two guests. The molar concentrations of the free guest are denoted by [H]and [G], respectively.

Equation(3) is noting also the relevant mass balance eqn (2), molar concentration of the 1 : 1 complex are denoted by [HG], [HG2] refers to 1 : 2 complex[1].

$$[H0] = [H] + [HG] + [HG2] \tag{2}$$

R= 0.9842, K_1=1225.8 (±0.312)M^{-1}, $K_2 = 2.654 \times 10^5 (\pm 0.312)M^{-2}$.

Reference:

[1] P. Thordarson, *Chem. Soc. Rev.*, 2011, **40**, 1305-1323.
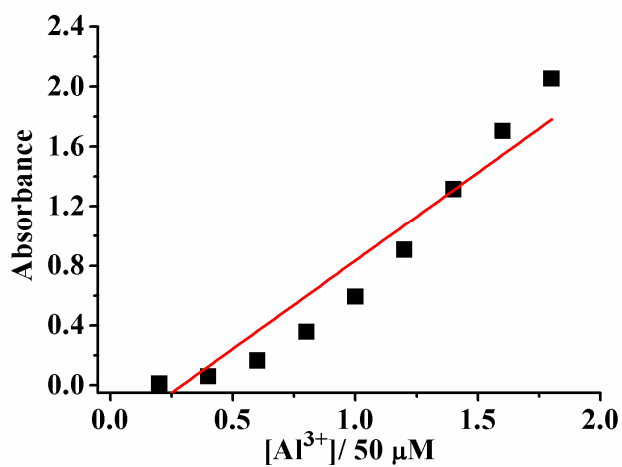
Figure S16. Absorbance calibration curve of probe **L1** (50 μM) at 558 nm as a function of Al^{3+} concentration in CH_3CN/H_2O (v/v, 98/2, pH 7) solution. Y = 1.184 X - 0.3483, R = 0.9055, LOD = 5.8 μM.
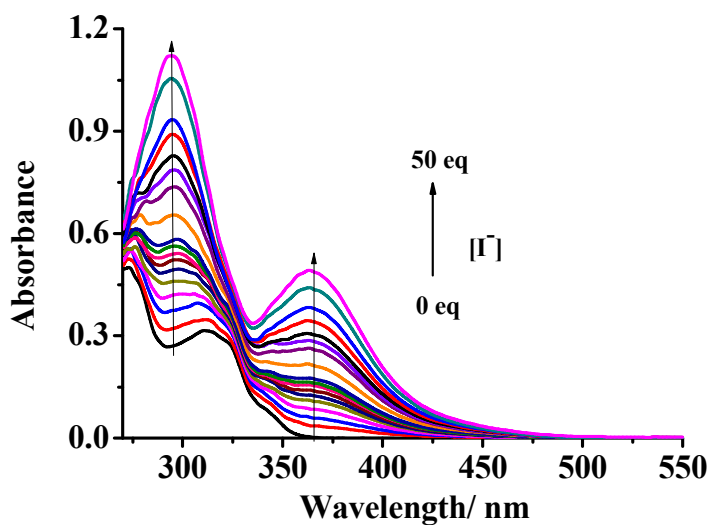
Figure S17. Absorption spectral changes of probe **L1** (10 μM, H_2O/1,4-dioxane, 1/99, v/v) solution upon addition of I^- (0 ~ 50 equiv.)
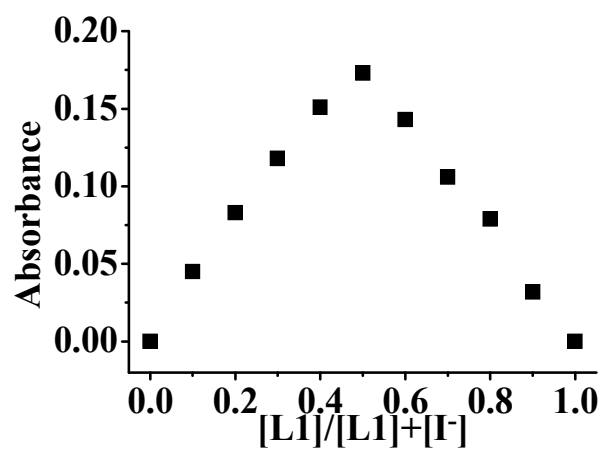
Figure S18. Job's plot data.
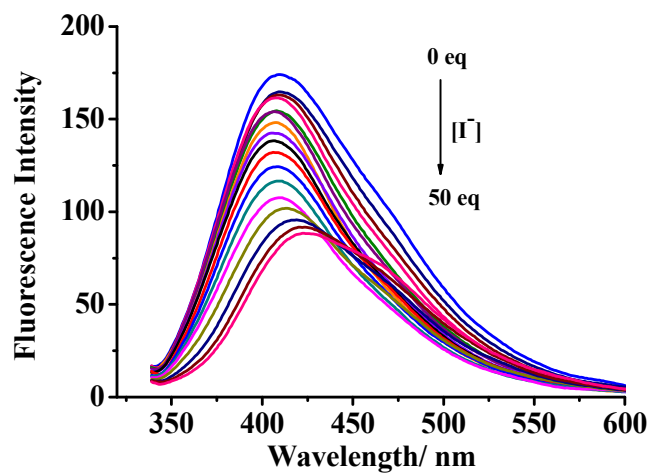
Figure S19. Fluorescence spectral changes of probe **L1** (10 μM, 1,4-dioxane/H_2O, v/v, 99/1) solution upon addition of I^- (0 ~ 500 μM); $\lambda_{ex}/\lambda_{em}$ = 315 nm/415 nm.
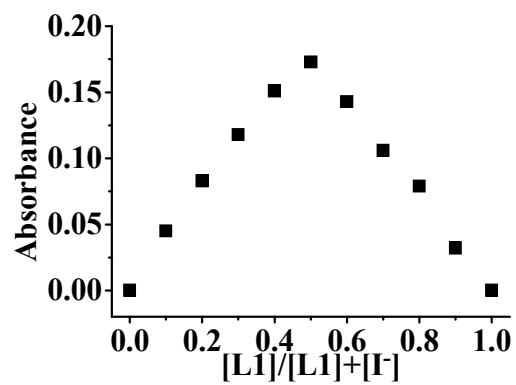
Figure S20. Job's plot data.
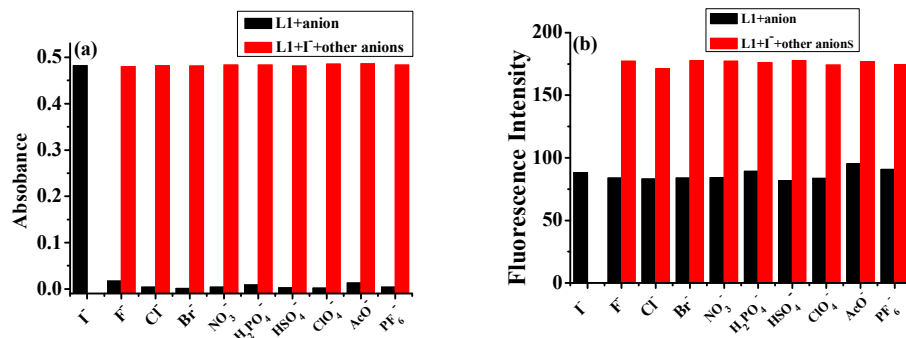
Figure S21. (a) Absorption response of probe **L1** (10 μM, 1,4-dioxane/H$_2$O, v/v, 99/1). Black bars: the absorbance of probe **L1** at 360 nm with the addition of the respective anions (50 eq.). White bars: the absorbance of probe **L1** at 360 nm with the addition of the respective competing anions (50 eq.) and I$^-$ (50 eq.); (b) Fluorescence response of probe **L1** (10 μM, 1,4-dioxane/H$_2$O, v/v, 99/1). Black bars: emission intensity of probe **L1** at 415 nm with the addition of the respective anios (50 eq.). White bars: emission intensity of probe **L1** at 415 nm with the addition of the respective competing anions (50 eq.) and I$^-$ (50 eq.). Anions including I$^-$, F$^-$, Cl$^-$, Br$^-$, NO$_3^-$, H$_2$PO$_4^-$, HSO$_4^-$, ClO$_4^-$, A$_C$O$^-$ and PF$_6^-$. λ$_{ex}$ = 315 nm
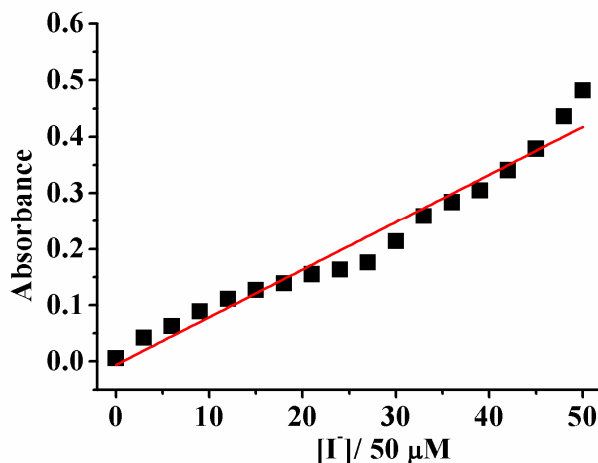
Figure S22.   Absorbance calibration curve of probe **L1** (10 μM) as a function of I$^-$ concentration in 1,4-dioxane/H$_2$O (v/v, 99/1) solution; λ$_{max}$ = 360 nm.

Y = 0.00847 X - 0.00598, R = 0.9578, LOD = 0.42 μM.
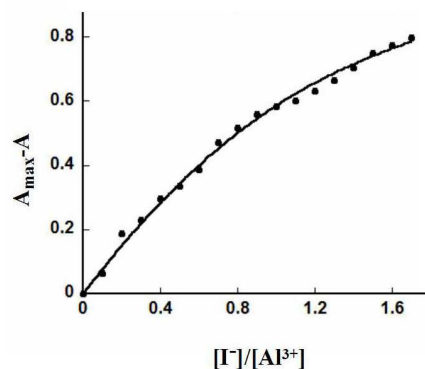
Figure S23. None-linear plot of probe **L1** (of probe **L1**(10 μM) assuming a 1:1 stoichiometry for association between probe **L1** and I^- in 1,4-dioxane/H_2O (v/v, 99/1) solution by absorption spectroscopy. λ_{max} = 360 nm.

The UV spectrum association constants of I^- were calculated by nonlinear fitting using the following formula [Eq. (4)]:

$$\Delta F = \frac{\Delta\beta([H]_0 + [G]_0 + \frac{1}{K_a}) \pm \sqrt{\Delta\beta^2([H]_0 + [G]_0 + \frac{1}{K_a})^2 - 4\Delta\beta^2[H]_0[G]_0}}{2} \tag{4}$$

where ΔI is the change in the fluorescence intensity of the L1 upon gradual addition of the I^-, and $\Delta\beta$ refers to the different molar absorptivity of the free host and the interaction complex. The total concentrations of host and guest are denoted by $[H]_0$ and $[G]_0$, respectively[1].

R = 0.9975, K = 2.08×10^5 (±0.005)M^{-1}

Reference:

[1] P. Thordarson, *Chem. Soc. Rev.*, 2011, **40**, 1305-1323.
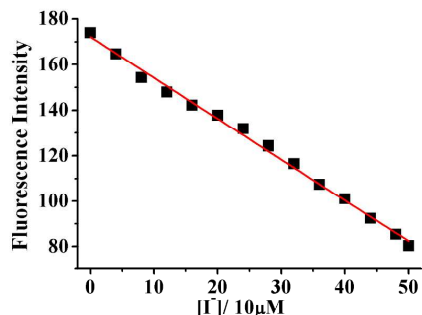
Figure S24. Fluorescence intensity calibration curve of probe **L1** (10 μM) as a function of I^- concentration in 1,4-dioxane/H_2O (v/v, 99/1) solution; $\lambda_{ex}/\lambda_{em}$ = 315 nm/415 nm.

Y = - 1.793 X + 172.1, R = 0.9953, LOD = 0.092 μM.
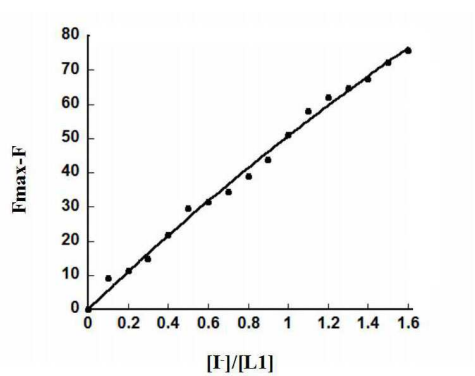
Figure S25. None-linear plot of probe**L1** (10 μM) assuming a 1:1 stoichiometry for association between probe **L1** and I^- in 1,4-dioxane/H_2O (v/v, 99/1) solution by fluorescence spectroscopy; $\lambda_{ex}/\lambda_{em}$ = 315 nm/415 nm.

The fluorescence spectrum association constants of I^- were calculated by nonlinear fitting using the following formula [Eq. (5)]:

$$\Delta I = \frac{\Delta a([H]_0 + [G]_0 + \frac{1}{K_a}) \pm \sqrt{\Delta a^2([H]_0 + [G]_0 + \frac{1}{K_a})^2 - 4\Delta a^2[H]_0[G]_0}}{2}$$

(5)

where ΔI is the change in the fluorescence intensity of the L1 upon gradual addition of the I^-, and Δα refers to the different constant of the free host and the interaction complex. The total concentrations of host and guest are denoted by $[H]_0$ and $[G]_0$, respectively[1].

R = 0.9910, K =1.04×10^4 (±0.033)M^{-1}

Reference:

[1] P. Thordarson, *Chem. Soc. Rev.*, 2011, **40**, 1305-1323.

Table S1. Comparison of probe **L1** and other probes in literature

	Our work	Ref. [2]	Ref. [3]	Ref. [4]	Ref. [5]
Detection ions	Al^{3+}, I^-	Al^{3+}	Al^{3+}	Al^{3+}	Al^{3+}
Detection solvent (v/v)	Al^{3+}: CH_3CN/H_2O (98/2) I^-: 1,4-dioxane/H_2O (99/1)	C_2H_5OH/H_2O (9/1)	CH_3OH/H_2O (1/1)	$C_2H_5OH/$ H_2O(95/5)	C_2H_5OH
Yield (%)	76.3	85.2	70.2	NA	93.1
Quantum yield	Al^{3+} 0.39	NA	0.076	0.102	NA
Detection limit (μM)	Al^{3+} 0.073 I^- 0.46	1.04	0.39	NA	0.2
Detection Method	Al^{3+}: Ratiometric fluorescence Stoke's shift (345 nm); FRET I^-: Fluorescence quenching PET	Ratiometric fluorescence Stoke's shift (143 nm)	Single wavelength Stoke's shift (72 nm); ESIPT	Single wavelength Stoke's shift (65 nm); PET	Single wavelength Stoke's shift (57 nm); PET
Application	PC3 Cells	Test strips	HeLa cells	NA	NA

	Ref. [6]	Ref.[7]	Ref.[8]
Detection ions	Al^{3+}, F^-	Al^{3+}	Al^{3+}
Detection solvent (v/v)	DMSO	CH_3CN	C_2H_5OH
Yield (%)	85.0	86.1	53
Quantum yield	Al^{3+}: 0.0198 F^-: 0.0182	NA	NA
Detection limit(μM)	Al^{3+}: 0.41 F^-: 14.36	0.42	0.22
Detection Method	Single wavelength Al^{3+}: ICT F^-: hydrogen bonded	Ratiometric fluorescence Stoke's shift (75 nm); ICT	Single wavelength; PET
Application	HeLa cells	HeLa cells	NA

[2] Y. Zhang , Y. Fang , N. Z. Xu, M. Q. Zhang, G. Z. Wu and C. Yao, *Chinese Chemical Letters*., 2016, **27**, 1673–1678.

[3] D. Sarkar, A. Pramanik, S. Biswas, P. Karmakar and T. K. Mondal, *RSC Adv*., 2014, **4,** 30666-30672.

[4] S. Samanta, B. Nath and J. B. Baruah, *Inorg. Chem. Commun*., 2012, **22**, 98-100.

[5] J. C. Qin, X. Y. Cheng, K. C. Yu, R. Fang, M. F. Wang and Z. Y. Yang 2015, **7**, 6799-6803.

[6] H. Y. Jeong, S. Y. Lee, J. Han, M. H. Lim and C. Kim, *Tetrahedron*., 2017, **73**, 2690-2697.

[7] R. Patil, A. Moirangthem, R. Butcher, N. Singh, A. Basu, K. Tayade, U. Fegade, D. Hundiwale and A. Kuwar, *Dalton Trans*., 2014, **43**, 2895-2899.

[8] J. W. Jeong, B. A. Rao and Y. A. Son, *Sensor. Actuators B: Chem*., 2015, **208** , 75-84.